

- [5] M. Ogawa, K. Ohata, T. Furutsuka, and N. Kawamura, "Submicron single-gate and dual-gate GaAs MESFET's with improved low noise and high gain performance," *IEEE Trans. Microwave Theory Tech.*, vol. MTT-24, pp. 300-305, June 1976.
- [6] H. Mizuno, "GaAs FET mount structure design for 30-GHz-band low noise amplifiers," *IEEE Trans. Microwave Theory Tech.*, vol. MTT-30, pp. 854-858, June 1982.

Measured Temperature-Dependence of Attenuation Constant and Phase Velocity of a Superconducting PbAu/SiO/Pb Microstripline at 10 GHz and 30 GHz

RALF PÖPEL

Abstract—Measured results for the temperature dependence of the attenuation constant and phase velocity of a superconducting microstripline at 10 GHz and 30 GHz are presented here for the first time. At 9.1 GHz the attenuation constant of a PbAu/SiO/Pb microstripline with a dielectric height of 880 nm decreases from 1.6 dB/m to 0.04 dB/m going from 4.2 K to 2.0 K, while at 27.3 GHz a decrease from 2.6 dB/m to 0.09 dB/m going from 3.0 K to 1.7 K was measured.

The calculated and measured temperature dependence of the phase velocity are in good agreement. The measured values for the attenuation constant together with the estimate of conductor losses from the Mattis-Bardeen theory, taking radiation losses and surface roughness into account, lead to an upper limit estimate for the loss factors of SiO.

I. INTRODUCTION

In contrast to waveguide technology, with the aid of stripline technology, circuits requiring a much smaller space and weighing considerably less can be constructed. Stripline circuits also have a lower heat conductivity and heat capacity. This is particularly advantageous for cryogenic microwave circuits. Moreover, cryogenic circuits with many planar and small Josephson elements can be placed on one substrate. Complex circuits can be built up in this way, e.g., logic circuits of Josephson computer technology [1], circuits with many dc series-connected Josephson elements for voltage standards [2], or Josephson arrays for microwave devices [3].

For low-temperature operation, stripline cross sections can be made considerably smaller than for use at room temperature [4]. Although with decreasing dielectric heights h the conductor losses for microstriplines increase considerably, the use of superconducting material for groundplane and strip can keep these losses down.

An advantage is that radiation losses which are important at frequencies ≥ 10 GHz for dielectric heights of the order of 0.5 mm decrease strongly with smaller dielectric heights.

For microstriplines with strip width $w \gg h$ the parallel plate

Manuscript received December 29, 1982; revised March 10, 1983. This work was supported in part by the Deutsche Forschungsgemeinschaft.

The author is with the Physikalisch-Technische Bundesanstalt, Bundesallee 100, West Germany.

line equation is valid in good approximation

$$Z_L = \frac{\eta}{\sqrt{\epsilon_r}} \cdot \frac{h}{w} \quad (1)$$

with $\eta = 120 \pi \Omega$ —wave impedance in free space, ϵ_r is the dielectric constant, h is the dielectric height, and w is the strip width.

From (1) we see that to obtain a definite wave impedance Z_L (e.g., for matching purposes), with smaller dielectric heights the strip width must also become smaller. Indeed, two strips can be placed closer together without any considerable coupling between them. These two effects allow a higher packing density to be achieved. Superconducting microstriplines of this kind have been examined both theoretically [5] and experimentally.

Kautz [6] has measured the attenuation constant α_0 of Nb/Nb₂O₅/PbAu microstriplines below 500 MHz and found a frequency independent Nb₂O₅ loss factor of about $2 \cdot 10^{-3}$ at 4 K. The temperature dependence of phase velocity has also been measured by Mason and Gould [7] on Ta/Ta-oxide/In microstriplines below 500 MHz. Because the superconducting microstriplines are for use at microwave frequencies or for picosecond pulse transmission, 10-GHz attenuation measurements of Nb/Nb₂O₅/PbAu lines were performed at 4.2 K [8]. The dielectric loss factor of Nb₂O₅ at 4.2 K was confirmed to be rather high, i.e., $\tan \delta \approx 2.1 \cdot 10^{-3}$. Because of an expected lower $\tan \delta$ of SiO and because the use of SiO is widespread in circuits with Josephson junctions [1], lines with SiO dielectric were examined. Measuring results are presented here for the temperature dependence of the attenuation constant α_0 and phase velocity v_p for a superconducting PbAu/SiO/Pb microstripline with a dielectric height of $h = 880$ nm at frequencies of about 10 GHz and 30 GHz. These results are discussed in conjunction with current theories.

II. THEORETICAL BACKGROUND

An investigation of superconductors with the help of resonant cavities is possible at microwave frequencies. The measured values of the surface resistance R_s can be approximated quite well by equations from the BCS theory if the energy gap 2Δ , or the mean free path l (of normal electrons), are used as approximation factors [9]. It is possible to measure the loss factors of dielectrics, inserted in a superconducting resonant cavity. In this way, Meyer [10] measured the loss factors of synthetic materials, such as quartz glasses and natural quartz, in the frequency range from 0.2 GHz to 7 GHz at temperatures between 2.0 K and 4.2 K. However, there are no measuring results of the surface resistance of PbAu and of the loss factor of SiO at microwave frequencies and low temperatures.

When we investigate a superconducting microstripline, according to the equation

$$\alpha_0 = A \cdot \alpha_c + \alpha_d + \alpha_r \quad (2)$$

conductor losses, dielectric losses, and radiation losses must be taken into account, where α_c , α_d , and α_r are the attenuation constants due to conductor losses, dielectric losses, and radiation losses, respectively. In addition, the factor A accounts for the influence of surface roughness.

In 1960, Swihart [5] derived formulas for calculating α_c , α_d , and the phase velocity v_p of superconducting microstriplines with $w \gg h$. These equations are the solutions of the classical model of superconductivity, namely of the two London equations, the two-fluid model, Maxwell's equations, isotropic material distribution,

and the local Ohm's law for the normal current density, which seems valid if the mean free path l is small compared to the classical skin depth δ , where

$$\delta = \frac{1}{[\omega \cdot \mu_0 \cdot \sigma/2]^{1/2}} \quad (3)$$

where μ_0 is the permeability of vacuum and σ is the normal conductivity. Also δ is small compared to the superconducting penetration depth λ .

Under the conditions

$$\omega \ll \frac{2\Delta_{a,b}}{\hbar} \quad (4)$$

where ω is the circular frequency, $2\Delta_{a,b}$ are the energy gaps, and \hbar is the Planck's constant divided by 2π , which is well satisfied at frequencies less than 100 GHz, and

$$\lambda_{a,b} \ll \frac{\delta_{a,b}}{4} \quad (5)$$

where $\lambda_{a,b}$ is the superconducting penetration depths, and a, b are the indices for characterization of metal ground plane and strip of microstripline.

The following formulas are obtained from [5]:

$$\begin{aligned} \alpha_c &= \mu_0 \frac{\omega^2}{C_0} \cdot \sqrt{\epsilon_r} \cdot \frac{1}{4h} \cdot [B]^{-1/2} \\ &\cdot \left\{ \sigma_{1a} \cdot \lambda_a^3 \left[\coth \left(\frac{d_a}{\lambda_a} \right) + \frac{da/\lambda a}{\sinh^2(d_a/\lambda_a)} \right] \right. \\ &\left. + \sigma_{1b} \cdot \lambda_b^3 \left[\coth \left(\frac{d_b}{\lambda_b} \right) + \frac{d_b/\lambda_b}{\sinh^2(d_b/\lambda_b)} \right] \right\} \\ v_\phi &= \frac{C_0}{\sqrt{\epsilon_r}} \cdot [B]^{-1/2} \\ \alpha_d &= \frac{\omega \cdot \tan \delta}{\alpha v_\phi} \end{aligned} \quad (6)$$

and

$$B = \left[1 + \frac{\lambda_a}{h} \cdot \coth \left(\frac{d_a}{\lambda_a} \right) + \frac{\lambda_b}{h} \cdot \coth \left(\frac{d_b}{\lambda_b} \right) \right]$$

where C_0 is the speed of light in vacuum, and $d_{a,b}$ are the metal film thicknesses. α_c doesn't depend on the wave impedance Z_L . σ_{1a} and σ_{1b} are the real components of a complex conductivity $\sigma = \sigma_1 - j\sigma_2$ in the superconducting state. v_ϕ is frequency-independent; we have a dispersion-free line. Compared to $C_0/\sqrt{\epsilon_r}$, v_ϕ is slowed down by the influence of the superconducting penetration depths. This influence becomes greater the nearer λ_a and λ_b get to the order of magnitude of the dielectric height h . The relation $v_\phi = f(\lambda_a, \lambda_b)$ can be used to measure the penetration depth. Henkels and Kircher [11] have done this on superconducting microstriplines with thin dielectric films below 25 MHz. They were able to confirm the coth dependence in (6).

In the following, the indices a and b are dropped for simplicity. The superconducting penetration depth is temperature-dependent according to the empirical function [12]

$$\lambda(T) = \frac{\lambda(0)}{\left[1 - (T/T_c)^4 \right]^{1/2}} \quad (7)$$

where T_c is the transition temperature.

With this, v_ϕ also changes with the temperature, which leads to a deviation of the resonant frequency of microstripline resonators.

To calculate the conductor attenuation constant α_c according to (6), we need values for the conductivity σ_1 of the normal current density in the superconducting state. In the two-fluid model, the simple relation

$$\frac{\sigma_1}{\sigma_n} = \left(\frac{T}{T_c} \right)^4 \quad (8)$$

is used; σ_n is the conductivity in the normal state at the transition temperature. According to [13], surface resistance is described better by formulas from the BCS theory than by using the two-fluid model. Kautz [14] suggested using the Mattis-Bardeen theory [15] to calculate σ_1/σ_n , which is based on the BCS theory and takes into account nonlocal behavior of current density and electrical field strength. In the extreme anomalous limit

$$\lambda \ll \xi_0 \quad (9)$$

where ξ_0 is the coherence length in pure material. For σ_1/σ_n they derived

$$\frac{\sigma_1}{\sigma_n} = \frac{2}{\hbar \omega} \int_{\Delta}^{\infty} \left[\frac{1}{1 + \exp \left(\frac{\epsilon}{kT} \right)} - \frac{1}{1 + \exp \left(\frac{\epsilon + \hbar \omega}{kT} \right)} \right] \cdot \frac{\epsilon^2 + \Delta^2 + \hbar \omega \epsilon}{(\epsilon^2 - \Delta^2)^{1/2} [(\epsilon + \hbar \omega)^2 - \Delta^2]^{1/2}} \cdot d\epsilon \quad (10)$$

for $\hbar \omega < 2\Delta$ where k is the Boltzmann constant.

Using approximation (4), Kautz gives an approximate expression for (10)

$$\frac{\sigma_1}{\sigma_n} = \frac{2\Delta}{kT} \cdot \frac{\exp(\Delta/kT)}{[1 + \exp(\Delta/kT)]^2} \cdot \ln(\Delta/\hbar \omega). \quad (11)$$

Further, he presents the equation

$$\lambda(0) = \left[\frac{\hbar}{\pi \cdot \mu_0 \cdot \Delta(0) \cdot \sigma_n} \right]^{1/2} \quad (12)$$

for calculating σ_n values from the values of the superconducting penetration depths. These are measured in [11], and can be extrapolated to $T = 0$ K.

For the temperature dependence of the energy gap, the equation

$$\Delta(T) = \Delta(0) \cdot \left\{ \cos \left[\frac{\pi}{2} \cdot \left(\frac{T}{T_c} \right)^2 \right] \right\}^{1/2} \quad (13)$$

is used here, which deviates from the more complicated BCS equation by a maximum of 2 percent.

Equation (6) with (7), (11)–(13) are used to calculate the expected attenuation behavior of the PbAu/SiO/Pb microstripline. The material parameters are listed in Table I, where bulk values are taken for the transition temperature and the energy gap, and $\epsilon_r = 5.7$ for SiO is taken from [16]. It can be seen that not all of the assumptions underlying the equations used are strictly fulfilled. $l \ll \lambda$ is not valid for either of the materials PbAu and Pb. So the applicability of (6) seems doubtful. However, σ_1 is introduced into (6) from a nonlocal theory through the use of (11). But this equation again is strictly valid only for $\lambda \ll \xi_0$ or $\lambda \ll \xi$, respectively, (ξ is the coherence distance in material with impurities), which is only satisfied for Pb and not for PbAu.

The theoretical results for α_c are therefore not expected to give exact values. But, to the authors knowledge, no more suitable formulas are yet available. Assuming that the violations of both conditions $l \ll \lambda$ and $\lambda \ll \xi$ lead to calculated values of α_c which

TABLE I
PARAMETERS OF MICROSTRIP LINE

	strip	ground plane	dielectric
Material	PbAu	Pb	SiO
T_c /K	7.2	7.2	
$2\Delta(\omega)/meV$	2.73	2.73	
$\epsilon_s/ S/m$	$2.423 \cdot 10^7$	$5.874 \cdot 10^7$	
$\lambda(\omega)/nm$	71.0	45.6	
$1(T_c)/nm; 1/4$	205	938	
$\{_0/nm$		10^3	
$\{/\mu m$	69		
ϵ_r			5.7
d/nm	450	450	
h/nm			880

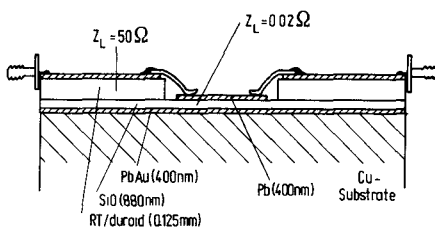


Fig. 1. Cu substrate with stripline structure built into the holder. 50- Ω line: $w = 0.5$ mm, $\epsilon_r = 2.2$; 0.02- Ω line: $w = 3.0$ mm, $\epsilon_r = 5.7$.

are too small, we can obtain a lower limit for α_c . In this way, calculated values for α_c will be presented in a later paragraph in conjunction with the measured results.

III. PRODUCTION OF MICROSTRIP LINE

The Cu substrates (Fig. 1), with the stripline structure, had the dimensions $36 \text{ mm} \times 10 \text{ mm} \times 1.5 \text{ mm}$. They were first polished mechanically and then chemically with strongly diluted FeCl_3 . In ultrasonic baths with dissolved soap, perethylenchloride, and acetone, all traces of grease were removed from the substrates, which were then freed from traces of oxide by immersion in dilute HCl . After this they were rinsed in an ultrasonic bath with distilled water. Water films evaporate when heated to 120°C under vacuum conditions. Insertion of the substrates into the vacuum chamber of the evaporation unit is done at this temperature.

The PbAu film and the SiO film were evaporated in one work process from two evaporation sources over the whole surface of the substrates at a pressure of $< 2.5 \cdot 10^{-6} \text{ mbar}$. The evaporation rate of Pb was about 1.5 nm/s followed by the evaporation of Au with a rate of 0.1 nm/s to 0.2 nm/s . Both metallic thin films interdiffused and made up the PbAu alloy. SiO tends to have inner stresses and to flake or rupture when cooled at liquid helium temperatures. It is essential that the SiO is annealed for more than one hour and to use high evaporation rates of the order of 2 nm/s [17].

Before evaporation of the Pb strip through a metal mask, the surface was sputtered clean with Ar. The Cu substrate used for microwave measurements with the stripline structure was cycled three times between 300 K and 4.2 K , and good adhesion of the structure was ascertained. The thickness of the SiO film of our specimen was roughly determined by a quartz thickness measurement during evaporation and later determined more exactly using an interference microscope to $h = 880 \text{ nm}$ with an uncertainty of

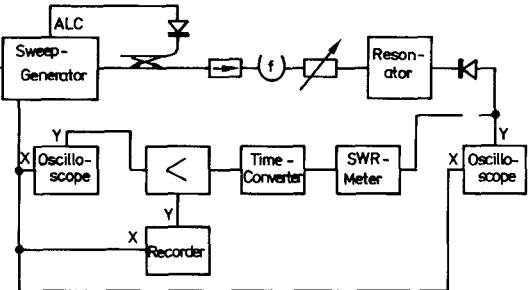


Fig. 2. Block diagram of measuring setup.

± 2 percent. The dimensions of the Pb strip were obtained by microscopic measurement to be $3.0 \text{ mm} \times 6.5 \text{ mm}$ (± 1 percent).

IV. MEASURING SETUP

Fig. 1 shows the Cu substrate with the stripline structure built into the holder. From the coaxial lines leading into the helium, transitions from $50\text{-}\Omega$ coaxial lines to $50\text{-}\Omega$ microstriplines follow. The dielectric of $50\text{-}\Omega$ microstriplines is formed by RT/duroid plates of thickness 0.125 mm , and the ground plane by Cu substrate with PbAu film. The influence of the SiO film on the wave impedance of $50\text{-}\Omega$ microstriplines is negligible, since the height of this film is much smaller than the height of the RT/duroid plates.

The resonator is contacted via bronze lugs, which also retain their elastic properties at low temperatures. The lugs are therefore soldered onto the strip of $50\text{-}\Omega$ microstriplines and carefully pressed onto the Pb strip. The coupling factor of the resonator is determined by the impedance steps between the microstriplines and the resonator.

As shown in Fig. 2, we measured the resonant frequencies f_0 with a frequency meter and fed the transmitted signal after detection to the vertical plates of an oscilloscope. The horizontal deflection is supplied by the sweep oscillator. From the curve so generated, we measured the 3-dB bandwidth Δf , whereby the detector diode operates in the quadratic region.

We were also able to amplify the detected signal with an SWR meter and to store it in a time converter. The stored curve can then be plotted by a recorder.

We used a 30-l helium container into which an insert containing 1 l of liquid helium was dipped. Temperatures lower than 4.2 K can be achieved in this insert by pumping with a vacuum pump. Temperatures can be maintained between $\pm 0.01 \text{ K}$ for a time interval of two minutes by a control valve. The temperature is measured by means of a calibrated carbon resistor using a four-point measurement.

V. MEASUREMENTS

Fig. 3(a) shows the recorded resonant curves of a microstrip resonator between 9.12 GHz and 9.2 GHz as the relative insertion loss measured at the outer connections of the coaxial lines leading into the helium container. With decreasing temperatures, the resonant frequency f_0 moves to higher frequencies, for lower temperatures more slowly. The unloaded quality factor Q_0 increases with decreasing temperature, therefore the coupling of the resonator with the input and output coupling factors $\beta_1 = \beta_2 = \beta$ becomes stronger.

Fig. 3(b) shows the form of the resonant curves at 27.3 GHz . Due to the stronger occurrence here of parasitic transmitted signals, the loaded quality factor Q_L could only be determined for temperatures below 3.0 K .

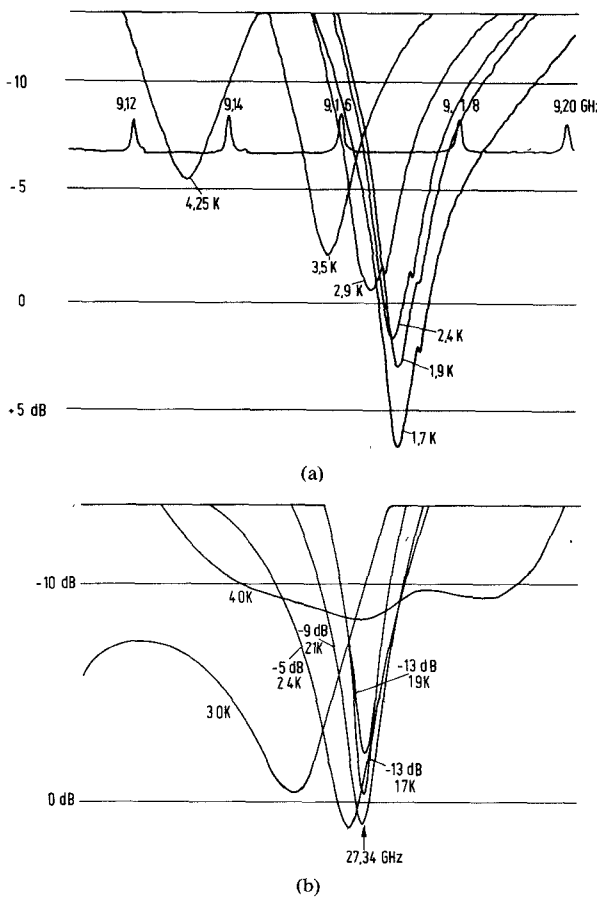


Fig. 3. Relative insertion loss of microstripline resonator at (a) 9.1 GHz and (b) 27.3 GHz (sweep width: 100 MHz).

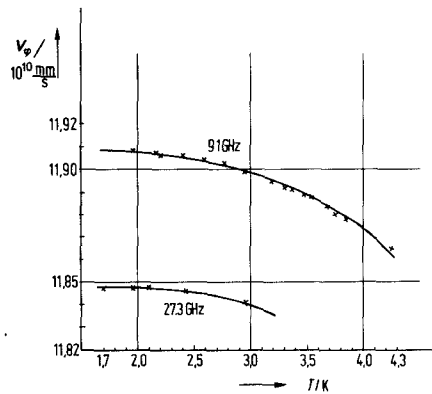


Fig. 4. Temperature dependence of phase velocity v_ϕ at 9.1 GHz and 27.3 GHz.

With f_0 measured, as well as the microscopically determined strip length L , the phase velocity v_ϕ can be determined by the equation

$$v_\phi = \frac{2 \cdot L \cdot f_0}{n} \quad (14)$$

where n is the resonant number.

The overall rms measuring uncertainty of v_ϕ is less than ± 1.4 percent. The crosses in Fig. 4 are the measuring points for v_ϕ , the curves are calculated according to (6) and (7) with the penetration depths given in Table I, and a selected dielectric constant $\epsilon_r = 5.64$ for 9.1 GHz. At 27.3 GHz, there is similarly good adjustment to the measuring points, assuming that $\epsilon_r = 5.7$.

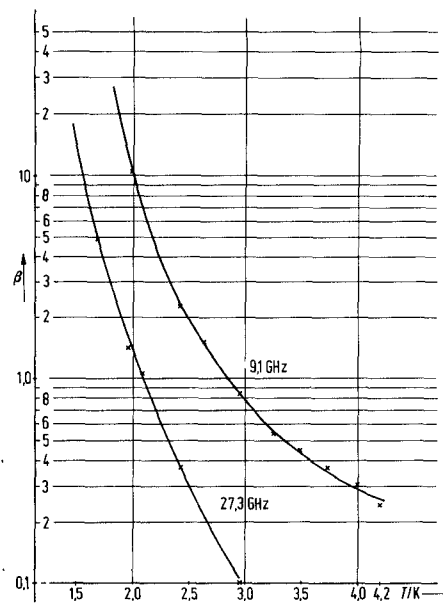


Fig. 5. Temperature dependence of coupling factors β at 9.1 GHz and 27.3 GHz.

At 9.17 GHz, and at the lowest temperature of 1.67 K which was reached, we measured an insertion loss of 2.25 dB between the outer connections of the coaxial lines. At this temperature, the coupling factors β become so large that the insertion loss of the resonator is negligible compared with the insertion loss of the coaxial lines. This was confirmed to within ± 0.25 dB by measuring the insertion loss of the coaxial lines with the holder replaced by a piece of coaxial line. In this way, the power ratios P_t/P_e (P_t is the transmitted power at resonator output, P_e is the incident power at resonator input) could be determined using the equation

$$\frac{P_t}{P_e} = \frac{4\beta^2}{(1+2\beta)^2}. \quad (15)$$

We then calculated the temperature dependence of the coupling factors, which are shown in Fig. 5. The load quality factors Q_L and the coupling factors β being known, the unloaded quality factors Q_0 follow from

$$Q_0 = (1+2\beta) \cdot Q_L \quad (16)$$

where

$$Q_L = \frac{f_0}{\Delta f}$$

and the attenuation constant of the dispersion-free line is

$$\alpha_0 = \frac{n \cdot \pi}{2 \cdot Q_0 \cdot L}. \quad (17)$$

The curves of the measured values for α_0 as a function of temperature at 9.1 GHz and 27.3 GHz are shown in Fig. 6. At 9.1 GHz the attenuation constant of the microstripline decreases from 1.6 dB/m to 0.04 dB/m going from 4.2 K to 2.0 K, while at 27.3 GHz a decrease from 2.6 dB/m to 0.09 dB/m going from 3.0 K to 1.7 K was measured. The same microstripline, but with good normal conductors (e.g., copper) instead of the superconductors, would exhibit nearly temperature-independent attenuation constants between 1.7 K and 4.2 K. They are in the order of 10^4 larger than those of the superconducting ones at 1.7 K. This high attenuation is caused by the small dielectric height. The measuring uncertainty increases from ± 7.5 percent to 14 percent

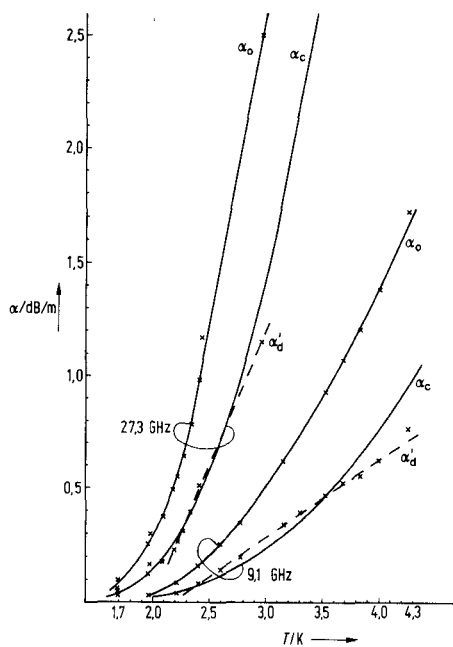


Fig. 6. Measured attenuation constants α_0 , estimated attenuation constant α_c and difference $\alpha'_d = \alpha_0 - \alpha_c$ at 9.1 GHz and 27.3 GHz

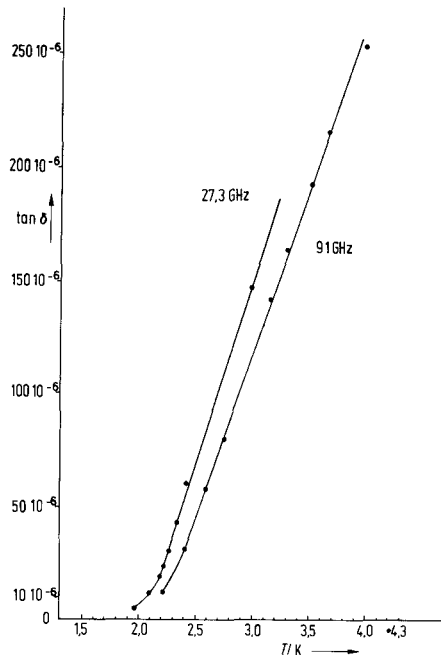


Fig. 7. Estimated upper limit of loss factors $\tan \delta$ at 9.1 GHz and 27.3 GHz.

at 9.1 GHz in the range of 4.2 K to 2.9 K and at 27.3 GHz in the range of 3.0 K to 2.1 K. The calculated curves of the conductor attenuation constants according to paragraph 2 are also shown. The curves $\alpha'_d = \alpha_0 - \alpha_c$ appear to show linear temperature-dependence above 2.4 K for 9.1 GHz and above 2.2 K for 27.3 GHz. Below these temperatures temperature-independent residual resistances and radiation losses affect α_0 . For our microstrip-line resonator, radiation losses can be calculated according to [18] as 0.01 dB/m at 9.1 GHz, and 0.08 dB/m at 27.3 GHz, independent of temperature.

For Cu substrates, an rms surface roughness of $R = 20$ nm was measured. With evaporated SiO film, the rms surface roughness increases to $R = 26$ nm. This value is smaller by a factor of 0.4 to 0.6 than the superconducting penetration depths. The influence

on factor A in (2) will be estimated by considering the analogy of rough surfaces of a normal conductor in the normal skin-effect region. For grooves parallel to the current direction, for $R/\delta = 0.5$ according to [19], $A = 1.1$ is the result. We therefore also take $A = 1.1$ for our present case. Then, a limit for the dielectric attenuation constants α_d , according to (2) and the accompanying loss factor $\tan \delta$ according to (6), can be estimated. This limit at 9.1 GHz and 27.3 GHz, as shown in Fig. 7, is strongly temperature-dependent.

VI. CONCLUSION

Measurements of an attenuation constant at microwave frequencies on a superconducting PbAu/SiO/Pb microstrip line with a dielectric height of 880 nm and theoretical estimates of the individual shares in the losses show that conductor losses and possibly dielectric losses comprise the largest part. Surface roughness has greater influence on the total attenuation constant than is the case for normal conductors, since, as a reference value, the superconducting penetration depths are the decisive factor and not the skin penetration depths.

By using superconductors with higher transition temperatures such as Nb or Nb₃Sn, dielectrics with low-loss factors such as SiO₂ or Al₂O₃, and of substrates with lower surface roughness, the attenuation constants of such microstrip lines can be considerably improved. In general, the use of superconducting microstrip lines with thin dielectrics at microwave frequencies is feasible.

ACKNOWLEDGMENT

The author wishes to thank J. Hinken for his advice and valuable help.

REFERENCES

- [1] W. Anacker, "Josephson computer technology: An IBM research project," *IBM J. Res. Develop.*, vol. 24, pp. 107-112, Mar. 1980.
- [2] R. L. Kautz and G. Costabile, "A Josephson voltage standard using a series array of 100 junctions," *IEEE Trans. Magn.*, vol. MAG-17, pp. 780-783, Jan. 1981.
- [3] A. K. Jain *et al.*, *Microwave Generation Using Coherent Arrays of Josephson Junctions, Squid '80*. New York: Walter de Gruyter, 1980, pp. 939-954.
- [4] R. L. Kautz, "Miniaturisation of normal-state and superconducting striplines," *J. Res. Nat. Bur. Stand.*, vol. 84(3), pp. 247-259, May-June 1979.
- [5] J. G. Swihart, "Field solution for a thin-film superconducting strip transmission line," *J. Appl. Phys.*, vol. 32, no. 3, pp. 461-469, Mar. 1961.
- [6] R. L. Kautz, "Attenuation in superconducting striplines," *IEEE Trans. Magn.*, vol. MAG-15, pp. 566-569, Jan. 1979.
- [7] P. V. Mason and R. W. Gould, "Slow-wave structures utilizing superconducting thin-film transmission lines," *J. Appl. Phys.*, vol. 40, no. 5, pp. 2039-2051, Apr. 1969.
- [8] R. Popel, "First measurement of a superconducting microstrip line attenuation constant at 10 GHz," to be published.
- [9] J. Halbritter, "On surface resistance of superconductors," *Z. Physik*, vol. 266, pp. 209-217, 1974.
- [10] W. Meyer, "Messung dielektrischer mikrowellenverluste bei tiefen temperaturen," Dissertation TU, Braunschweig, 1977.
- [11] W. H. Henkels and C. J. Kircher, "Penetration depth measurements on Type II superconducting films," *IEEE Trans. Magn.*, vol. MAG-13, pp. 63-66, Jan. 1977.
- [12] M. Tinkham, *Superconductivity, Low Temperature Physics*. New York: de Witt Dreyfus and de Gennes, 1962, p. 156.
- [13] E. Voges and K. Petermann, "Losses in superconducting coaxial transmission lines," *Arch. Elek. Übertragung*, vol. 27, pp. 384-388, Sept. 1973.
- [14] R. L. Kautz, "Picosecond pulses on superconducting striplines," *J. Appl. Phys.*, vol. 49, no. 1, pp. 308-314, Jan. 1978.
- [15] D. C. Mattis and J. Bardeen, "Theory of the anomalous skin effect in normal and superconducting metals," *Phys. Rev.*, vol. 111, no. 2, pp. 412-417, July 1958.
- [16] J. H. Greiner *et al.*, "Fabrication process for Josephson integrated circuits," *IBM J. Res. Develop.*, vol. 24, pp. 195-205, Mar. 1980.
- [17] A. E. Hill and G. R. Hoffmann, "Stress in films of silicon monoxide," *Brit. J. Appl. Phys.*, vol. 18, pp. 13-22, 1967.
- [18] E. Belohoubek and E. Denlinger, "Loss considerations for microstrip resonators," *IEEE Trans. Microwave Theory Tech.*, vol. MTT-23, pp. 522-526, June 1975.
- [19] S. P. Morgan, "Effect of surface roughness on eddy current losses at microwave frequencies," *J. Appl. Phys.*, vol. 20, pp. 352-362, Apr. 1949.